ARTICLE
Journal of Cellular Biochemistry 115:1403–1411 (2014)

Journal of Cellular Biochemistry

Cytoprotective Effect of Eckol Against Oxidative Stress-Induced Mitochondrial Dysfunction: Involvement of the FoxO3a/AMPK Pathway

Areum Daseul Kim,[1] Kyoung Ah Kang,[1] Mei Jing Piao,[1] Ki Cheon Kim,[1] Jian Zheng,[1] Cheng Wen Yao,[1] Ji Won Cha,[1] Chang Lim Hyun,[1] Hee Kyoung Kang,[1] Nam Ho Lee,[2] and Jin Won Hyun[1]*

[1]*School of Medicine, Jeju National University, Jeju 690-756, Korea*

[2]*Department of Chemistry, College of Natural Sciences, Jeju National University, Jeju 690-756, Korea*

ABSTRACT

This study investigated the cytoprotective effect of *Ecklonia cava*-derived eckol against H_2O_2-induced mitochondrial dysfunction in Chang liver cells. While H_2O_2 augmented levels of mitochondrial reactive oxygen species (ROS), eckol decreased it. Eckol also attenuated high intracellular Ca^{2+} levels stimulated by H_2O_2 and recovered H_2O_2-diminished ATP levels and succinate dehydrogenase activity. Eckol time-dependently increased the expression of manganese superoxide dismutase (Mn SOD), a mitochondrial antioxidant enzyme with cytoprotective effect against oxidative stress. Eckol recovered Mn SOD expression and activity that were decreased by H_2O_2. Finally, eckol induced Mn SOD through phosphorylated AMP-activated protein kinase (AMPK) and forkhead box O3a (FoxO3a). Specific silencing RNAs (siRNAs) against FoxO3a and AMPK reduced eckol-stimulated Mn SOD expression, and diethyldithiocarbamate (Mn SOD inhibitor) and siRNA against Mn SOD reduced the cytoprotective effect of eckol against H_2O_2-provoked cell death. These results demonstrate that eckol protects cells from mitochondrial oxidative stress by activating AMPK/FoxO3a-mediated induction of Mn SOD. J. Cell. Biochem. 115: 1403–1411, 2014.

KEY WORDS: ECKOL; MANGANESE SUPEROXIDE DISMUTASE; FORKHEAD BOX O3a; AMP-ACTIVATED PROTEIN KINASE; CYTOPROTECTION

Reactive oxygen species (ROS), including superoxide anions, hydrogen peroxide (H_2O_2), and hydroxyl radicals, are produced as by-products of normal cellular metabolism [Devasagayam et al., 2004]. At above-normal levels, ROS can cause irreversible cellular injury and dysfunction by directly oxidizing and damaging DNA, proteins, and lipids. These modifications to cellular macromolecules are associated with the underlying pathogenesis of ROS-mediated oxidative stress [Balaban et al., 2005]. High concentrations of ROS alter the balance of endogenous protective versus apoptotic systems and result in mitochondrial dysfunction. Calcium ions and other apoptosis-related and regulatory factors are then released from damaged mitochondria into the cytosol following oxidative disruption of the mitochondrial membrane [Richter, 1993].

Manganese superoxide dismutase (Mn SOD), the primary antioxidant enzyme responsible for scavenging superoxide anions in the mitochondria, is essential for the survival of all aerobic organisms [Weisiger and Fridovich, 1973]. Under-expression of Mn SOD is now being investigated as a causative factor in various pathologies, including myriad neurological disorders and cancer [Oberley and Buettner, 1979; Marcus et al., 2006]. On the other hand, overexpression of Mn SOD protects cells against oxidative stress-induced cell death and tissue injury [Kiningham et al., 1999].

Forkhead box O (FoxO) proteins are transcription factors that are involved in the detoxification of ROS, DNA repair, apoptosis, and cell-cycle arrest [Kiningham et al., 1999; Tran et al., 2002; Ghaffari et al., 2003]. The FoxO family consists of FoxO1, FoxO3a, FoxO4, and FoxO6a. These transcription factors activate target genes by binding to the consensus binding motif TTGTTTAC [Monsalve and Olmos, 2011].

The FoxO3a mediates transcriptional up-regulation of the ROS scavenging enzymes superoxide dismutase 2 (also known as Mn

Grant sponsor: Korean Government (Ministry of Education, Science and Technology); Grant number: NRF-C1ABA001-2011-0021037.
*Correspondence to: Jin Won Hyun, School of Medicine, Jeju National University, Jeju 690-756, Korea. E-mail: jinwonh@jejunu.ac.kr
Manuscript Received: 1 December 2013; Manuscript Accepted: 14 February 2014
Accepted manuscript online in Wiley Online Library (wileyonlinelibrary.com): 18 February 2014
DOI 10.1002/jcb.24790 • © 2014 Wiley Periodicals, Inc.

SOD) and catalase [Kops et al., 2002]. The activation of FoxO3a is mediated by translational modifications (e.g., phosphorylation, acetylation, ubiquitination, and methylation) [Zhao et al., 2011]. FoxO3a activity is evoked by the AMP-activated protein kinase (AMPK) pathway, an important signaling pathway involved in ROS regulation. AMPK phosphorylates FoxO3a at six sites (Thr179, Ser399, Ser413, Ser555, Ser588, and Ser626), leading to the stimulation of FoxO3a transcriptional functions [Greer et al., 2007]. Recently, AMPK1α was found to be required for FoxO3a-dependent transcription of Mn SOD, catalase, gamma-glutamylcysteine synthase, and thioredoxin [Li et al., 2009].

Eckol is a trimeric phloroglucinol with a dibenzeno-1,4-dioxin skeleton. This compound is one of the major phlorotannins derived from *Ecklonia cava*, a brown alga belonging to the *Laminariaceae* family that is abundant in the subtidal regions of Jeju Island (Korea). Recently, we demonstrated that eckol exerts cytoprotective properties against oxidative stress [Kang et al., 2005; Moon et al., 2008; Zhang et al., 2008; Piao et al., 2012], up-regulates heme oxygenase-1 via activation of extracellular signal-regulated kinase (Erk) and phosphoinositide 3-kinase [Kim et al., 2010], and inhibits the maintenance of stemness in glioma stem-like cells, along with associated malignancies [Hyun et al., 2011]. The present study demonstrated the ability of eckol to safeguard mitochondria against oxidative stress-damaged hepatocytes in terms of the AMPK/FoxO3a/Mn SOD pathway. Therefore, the hepatoprotective activity of eckol may be useful for developing its preventive or therapeutic medicine.

MATERIALS AND METHODS

REAGENTS

Eckol was provided by Professor Nam Ho Lee (Jeju National University, Jeju, Korea). The chemical structure characterization of eckol was accomplished by the inspection of spectroscopic data including nuclear magnetic resonance spectra as well as by the comparison of the data to the literature [Fukuyama et al., 1985]. The purity of the isolate was over 90% based on HPLC analysis. Eckol was dissolved in dimethyl sulfoxide (DMSO) and final concentration of DMSO in control or eckol treatment did not exceed the 0.05%. (3-(4,5-Dimethylthiazol-2-yl)-2,5-diphenyltetrazolium) bromide (MTT) and diethyldithiocarbamate (DEDTC) were purchased from Sigma-Aldrich Corporation (St. Louis, MO). Dihydrorhodamine 123 (DHR 123) and Rhod-2 acetoxymethyl ester (Rhod-2 AM) were purchased from Molecular Probes (Eugene, OR). Compound C was purchased from Calbiochem Co. (San Diego, CA). Anti-phospho AMPKα (Thr 172), anti-AMPKα, and anti-FoxO3a antibodies were purchased from Cell Signaling Technology (Beverly, MA). The anti-phospho serine/threonine antibody was purchased from Abcam (Cambridge, MA), and the anti-Mn SOD antibody was purchased from Stressgen Biotechnologies Corporation (Victoria, Canada).

CELL CULTURE

The human hepatocyte-derived Chang liver cell line was obtained from the American type culture collection (Rockville, MD). Cells were maintained at 37°C in an incubator with a humidified atmosphere of 5% CO_2 in air. Cells were cultured in RPMI 1640 medium containing 0.1 mM non-essential amino acids, 10% heat-inactivated fetal calf serum, streptomycin (100 μg/ml), and penicillin (100 units/ml).

MITOCHONDRIAL ROS MEASUREMENTS

DHR 123 is a dye freely diffusing into cells, oxidized primarily by H_2O_2 in a myeloperoxidase-dependent reaction to green fluorescence. As DHR 123 is accumulated by mitochondria, the production of ROS at the mitochondrial level can be detected [Banki et al., 1999]. Cells were seeded into a coverslip-loaded, six-well plate at a density of 1×10^5 cells/ml. At 16 h after plating, cells were treated with eckol (10 μg/ml) for 1 h, followed by H_2O_2 (600 μM) and incubated for 30 min. After changing the cell culture medium, DHR 123 (20 μM) was added to each well and the plate was incubated for an additional 30 min at 37°C. The stained cells were washed with phosphate-buffered saline (PBS) and mounted onto a microscope slide in mounting medium (DAKO, Carpinteria, CA). Images were collected by using the Laser Scanning Microscope 5 PASCAL program (Carl Zeiss, Jena, Germany) and a confocal microscope. Mitochondrial ROS were also detected by using a FACSCalibur flow cytometer (Becton Dickinson, Franklin Lakes, NJ). Cells were loaded with DHR 123 for 30 min at 37°C, as described above. The supernatant was then removed by suction, and the cells were trypsinized for removal from the coverslips. After trypsin treatment, the DHR 123-loaded cells were washed with PBS, and the fluorescence was measured via flow cytometry. In addition, the cells were seeded into a 96-well plate at a density of 1×10^5 cells/ml. At 16 h after plating, the cells were treated with eckol. One hour later, H_2O_2 was added to the plate, and cells were incubated for another 30 min at 37°C. After the addition of 20 μM DHR 123 for 10 min, fluorescence was detected by using a Perkin Elmer LS-5B spectrofluorometer (Perkin Elmer, Waltham, MA).

MITOCHONDRIAL Ca^{2+} MEASUREMENTS

Rhod-2 AM was used to measure mitochondrial Ca^{2+} levels. This dye has a net positive charge, which facilitates its sequestration into the mitochondria due to membrane potential-driven uptake. The AM ester of the probe is cleaved in the cytosol, and taken up into the mitochondria to yield the Rhod-2 indicator [Colombaioni et al., 2002]. The fluorescence intensity after mitochondrial labeling was measured by using confocal microscopy and flow cytometry. Cells were seeded into a coverslip-loaded, six-well plate at a density of 1×10^5 cells/ml. At 16 h after plating, cells were treated with eckol. H_2O_2 was added 1 h later, and the cells were incubated for another 24 h. Rhod-2 AM was then added to each well, and the plate was incubated for an additional 15 min at 37°C. After washing with PBS, the stained cells were mounted onto a microscope slide in mounting medium (DAKO). Images were collected by using the laser scanning microscope 5 PASCAL program (Carl Zeiss) and a confocal microscope. For flow cytometric analysis, cells were seeded into a six-well plate at a density of 1×10^5 cells/ml, and were treated with eckol 16 h later. After 1 h, H_2O_2 was added to each well, and the cells were incubated for an additional 24 h. Cells were harvested, washed, and suspended in PBS containing Rhod-2 AM (20 μM). After 15 min of incubation at 37°C, the cells were washed and suspended in PBS. The fluorescence of the Rhod-2 AM-loaded cells was measured by using a flow cytometer.

QUANTIFICATION OF CELLULAR ATP LEVELS

Mitochondrial function was evaluated by measuring cellular ATP production in Chang liver cells. Cells were harvested and washed twice with PBS. The harvested cells were then lysed on ice for 30 min in lysis buffer I (200 μl; 25 mM Tris (pH 7.8), 270 mM sucrose, and 1 mM EDTA), followed by sonication (3 × 15 s) and centrifugation at 4°C for 10 min at 16,000g. The supernatants were collected from the lysates, and ATP content was assayed by using a luciferase/luciferin ATP determination kit (Molecular Probes), as described previously [Connop et al., 1999].

MITOCHONDRIAL SUCCINATE DEHYDROGENASE ACTIVITY

Mitochondrial function was also evaluated by using the MTT assay [Carmichael et al., 1987], which was customized for the assessment of mitochondrial succinate dehydrogenase activity [Alley et al., 1988]. Cells were seeded into a 96-well plate at a density of 1×10^5 cells/ml. At 16 h after plating, the cells were treated with eckol for 1 h, followed by the addition of H_2O_2 and incubation for an additional 24 h at 37°C. MTT stock solution (50 μl; 2 mg/ml) was then added to each well to yield a total reaction volume of 200 μl. After incubation for a further 4 h, the plate was centrifuged at 800g for 5 min, and the supernatants were aspirated. The formazan crystals in each well were dissolved in DMSO (150 μl), and the A_{540} was read on a scanning multi-well spectrophotometer.

REVERSE TRANSCRIPTASE PCR (RT-PCR)

Total RNA was isolated from the cells with Trizol (GibcoBRL, Grand Island, NY). PCR conditions for amplification of Mn SOD and the housekeeping gene, glyceraldehyde 3-phosphate dehydrogenase (GAPDH), were as follows: 30 cycles of melting at 94°C for 15 s; annealing at 60°C for 30 s; and elongation at 68°C for 60 s. The primer pairs (Bionics, Seoul, Korea) were as follows (forward and reverse, respectively): Mn SOD, forward 5′-GACCTGCCTTACGACTATGG-3′ and reverse 5′-GACCTTGCTCCTTATTGAAG-3′, 600 bp; and GAPDH, forward 5′-GTGGGCCGCCCTAGGCACCAGG-3′ and reverse 5′-GGAGGAAGAGGATGCGGCAGTG-3′, 1,054 bp. Amplified products were resolved by electrophoresis in 1% agarose gels, stained with ethidium bromide, and photographed under ultraviolet light.

WESTERN BLOT ANALYSIS

Harvested cells were lysed on ice for 30 min in lysis buffer (100 μl; 120 mM NaCl, 40 mM Tris (pH 8), and 0.1% NP40) and centrifuged at 13,000g for 15 min. The supernatants were collected from the lysates, and the protein concentrations were measured. Aliquots of the lysates (40 μg of protein) were boiled for 5 min and electrophoresed in a 10% sodium dodecyl sulfate (SDS)–polyacrylamide gel. The electrophoresed proteins were then transferred onto nitrocellulose membranes and subsequently incubated with primary antibodies against Mn SOD, phospho AMPKα (Thr 172), AMPKα, and FoxO3a. The membranes were further incubated with secondary anti-immunoglobulin-G-horseradish peroxidase conjugates (Pierce, Rockford, IL), followed by exposure to X-ray film. The protein bands were detected by using an enhanced chemiluminescence Western blotting detection kit in accordance with the manufacturer's instructions (Amersham, Little Chalfont, Buckinghamshire, UK).

MEASUREMENT OF Mn SOD ACTIVITY

Cells were seeded into a culture dish at a density of 1×10^5 cells/ml and treated with eckol at 16 h after plating. After incubation with eckol for 1 h, H_2O_2 was added to the plate, and the cells were incubated for a further 24 h. The cells were then washed with cold PBS and scraped off the plate. The harvested cells were suspended in 10 mM phosphate buffer (pH 7.5) and lysed on ice by sonication (2 × 15 s). Triton X-100 (1%) was added to the lysates and samples were then incubated for 10 min on ice. The lysates were clarified by centrifugation at 5,000g for 10 min at 4°C to remove cellular debris. The protein content of the supernatant was determined by the Bradford method, with bovine serum albumin employed as the standard. The level of epinephrine auto-oxidation inhibition was assessed to detect Mn SOD activity [Misra and Fridovich, 1972]. Fifty micrograms of cell supernatant were added to 500 mM phosphate buffer (pH 10.2) containing 1 mM potassium cyanide (an inhibitor of Cu/Zn SOD) and 1 mM epinephrine. Epinephrine rapidly undergoes auto-oxidation at pH 10 to produce the pink-colored adrenochrome product, which was assayed at 480 nm by using an ultraviolet/visible spectrophotometer in the kinetic mode. The rate of epinephrine auto-oxidation inhibition by Mn SOD was monitored at 480 nm, and the amount of enzyme required to produce 50% inhibition was defined as 1 unit of enzyme activity. Mn SOD activity was expressed as units per milligram of protein.

IMMUNE-PRECIPITATION

Harvested cells were washed with PBS and lysed in immune-precipitation buffer (1 ml; 50 mM Tris–HCl (pH 6.8), 0.1% SDS, 150 mM NaCl, 1 mM EDTA, 0.1 mM Na_3VO_4, 1 mM sodium fluoride, 1% Triton X-100, 1% NP40, 1 mM dithiothreitol, 1 mM PMSF, 1 μg/ml aprotinin, and 1 μg/ml leupeptin). After lysis for 30 min and centrifugation at 14,000g for 15 min, the supernatants were collected. An aliquot of protein G agarose beads was added to the immune-precipitation buffer. Cell lysates were subjected to immune-precipitation with an anti-FoxO3a antibody, followed by an agarose-conjugated secondary antibody. Western blotting analysis was then performed with an antibody against phospho serine/threonine.

IMMUNOCYTOCHEMISTRY

Cells plated on coverslips were fixed with 4% paraformaldehyde for 30 min and permeabilized with PBS containing 0.1% Triton X-100 for 2.5 min. Cells were subsequently treated with blocking medium (PBS containing 3% bovine serum albumin) for 1 h and incubated with the anti-FoxO3a antibody diluted in blocking medium for 2 h. The bound anti-FoxO3a antibody was detected by reaction for 1 h with a fluorescein isothiocyanate-conjugated secondary antibody (1:500 dilution; Jackson Immuno Research Laboratories, West Grove, PA). After washing with PBS, stained cells were mounted onto microscope slides in mounting medium containing 4′,6-diamidino-2-phenylindole (Vector, Burlingame, CA). Images were collected by using the LSM 510 program on a Zeiss confocal microscope.

TRANSIENT TRANSFECTION OF SMALL INTERFERING RNA (siRNA)

Cells were seeded at a density of 1.5×10^5 cells/ml in a 24-well plate and allowed to reach approximately 50% confluency on the day of

transfection. The control mismatched siRNA construct (siControl RNA) was obtained from Santa Cruz Biotechnology (Santa Cruz, CA), whereas siRNAs against FoxO3a (siFoxO3a RNA), AMPK (siAMPK RNA), and Mn SOD (siMn SOD RNA) were purchased from Bioneer Corporation (Daejon, Korea). Cells were transfected with 10–50 nM of each siRNA by using lipofectamine^{TM} 2000 (Invitrogen, Carlsbad, CA) according to the manufacturer's instructions.

CELL VIABILITY ASSAY

The effect of eckol on cell viability was determined by employing the MTT assay [Carmichael et al., 1987]. Cells were seeded into a 96-well plate at a density of 1×10^5 cells/ml and pretreated with 10 μM DEDTC (10 μM; a selective inhibitor of Mn SOD) for 30 min, followed incubation with eckol for 1 h, and subsequent exposure to H_2O_2 for 24 h at 37°C. MTT stock solution (50 μl, 2 mg/ml) was added to each well to attain a total reaction volume of 200 μl. After incubation for another 2.5 h, the supernatants were aspirated. The formazan crystals in each well were dissolved in DMSO (150 μl), and the absorbance at 540 nm was read on a scanning multi-well spectrophotometer.

STATISTICAL ANALYSIS

All measurements were made in triplicate, and all values are expressed as the mean ± the standard error. Data were analyzed by applying an analysis of variance, followed by Tukey's post hoc test. In all cases, $P < 0.05$ was considered statistically significant.

RESULTS

ECKOL DECREASES H_2O_2-INDUCED MITOCHONDRIAL ROS LEVELS

We have previously reported the radical scavenging effects of eckol at 0.1, 1, and 10 μg/ml on the DPPH radical and hydroxyl radical showed the highest effect at 10 μg/ml [Kang et al., 2005]. Therefore,

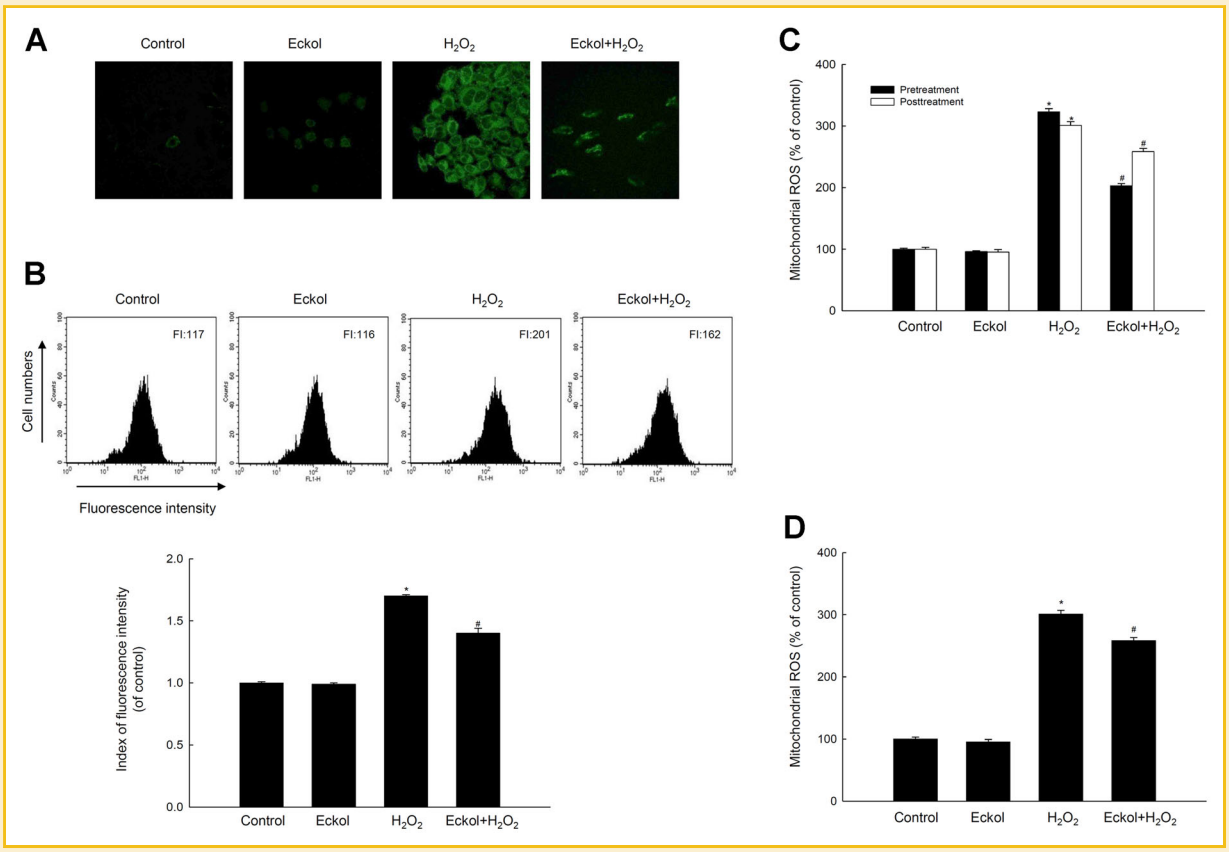

Fig. 1. Effect of eckol on H_2O_2-induced mitochondrial ROS generation. Pretreatment of eckol indicates that cells were treated with eckol (10 μg/ml) for 1 h, followed by H_2O_2 (600 μM) for 30 min. Post-treatment of eckol indicates that cells were treated with by H_2O_2 for 30 min, followed by eckol for 1 h. After changing the cell culture medium, DHR 123 (20 μM) was added and the cells were incubated for an additional 30 min at 37°C. A: Representative confocal images illustrated the increase in the green fluorescence intensity of DHR 123 generated by the elevated ROS levels in H_2O_2-treated cells compared with the untreated control, eckol-treated, and eckol-pretreated and H_2O_2-treated cells (magnification 400×). B: Mitochondrial ROS levels in pretreatment of eckol were also quantified in harvested cells by flow cytometry (FI, fluorescence intensity of DHR 123) after the addition of DHR123. *Significantly different from untreated control cells ($P < 0.05$), and #significantly different from H_2O_2-treated cells ($P < 0.05$). C: ROS levels in pretreatment of eckol and post-treatment of eckol were detected by spectrofluorometry after the addition of DHR123. *Significantly different from untreated control cells ($P < 0.05$), and #significantly different from H_2O_2-treated cells ($P < 0.05$). D: Cells were treated with eckol for 5 h to fully penetrate eckol into cells. And the cells were washed and changed by medium, and H_2O_2 was treated for 30 min. ROS levels were detected by spectrofluorometry after the addition of DHR123. *Significantly different from untreated control cells ($P < 0.05$), and #significantly different from H_2O_2-treated cells ($P < 0.05$).

10 μg/ml of eckol was chosen as optimal dose in these studies. And we also reported that the cell viability at different concentrations of H_2O_2 (200–1,000 μM) in Chang liver cell line was assessed by using MTT test. The cell viability was decreased in concentration-dependent manner, and H_2O_2 at 600 μM showed the value of 50% inhibition of cell growth [Zhang et al., 2010]. Thus, we chose H_2O_2 at 600 μM as optimal concentration in these studies.

Mitochondrial ROS generated by H_2O_2 were detected by using DHR 123 fluorescent dye. Analysis of confocal microscopy images revealed that H_2O_2 treatment increased mitochondrial ROS levels relative to the untreated and eckol-only controls, whereas eckol decreased the green fluorescence intensity of H_2O_2-induced mitochondrial ROS (Fig. 1A). In addition, flow cytometric detection of mitochondrial ROS revealed a fluorescence intensity value of 162 (index 1.4) in eckol-pretreated and H_2O_2-treated cells, compared with fluorescence intensity values of 117 (index 1) in untreated control cells, 116 (index 1) in eckol-treated cells, and 201 (index 1.7) in H_2O_2-treated cells (Fig. 1B). The fluorescence spectrometry data likewise revealed that H_2O_2 increased mitochondrial ROS levels. However, pretreatment with eckol ameliorated the H_2O_2-provoked increase in ROS content (Fig. 1C). The post-treatment with eckol in H_2O_2-treated cells suppressed ROS content (Fig. 1C). Eckol and H_2O_2 can react in the cell media via the direct ROS scavenging ability of eckol [Kang et al., 2005]. Therefore, pretreated cells with eckol were washed out and changed the fresh medium. Then after H_2O_2 treatment in eckol-washed out cells, ROS levels were detected. The H_2O_2 treatment in eckol-washed out cells showed the low levels of ROS compared to only H_2O_2-treated cells, suggesting that eckol penetrated into cells and scavenged cellular ROS (Fig. 1D).

ECKOL ATTENUATES ROS-GENERATED MITOCHONDRIAL CA^{2+} LEVELS

ROS levels augmented by environmental stress can in turn elevate mitochondrial Ca^{2+} levels, leading to mitochondrial dysfunction

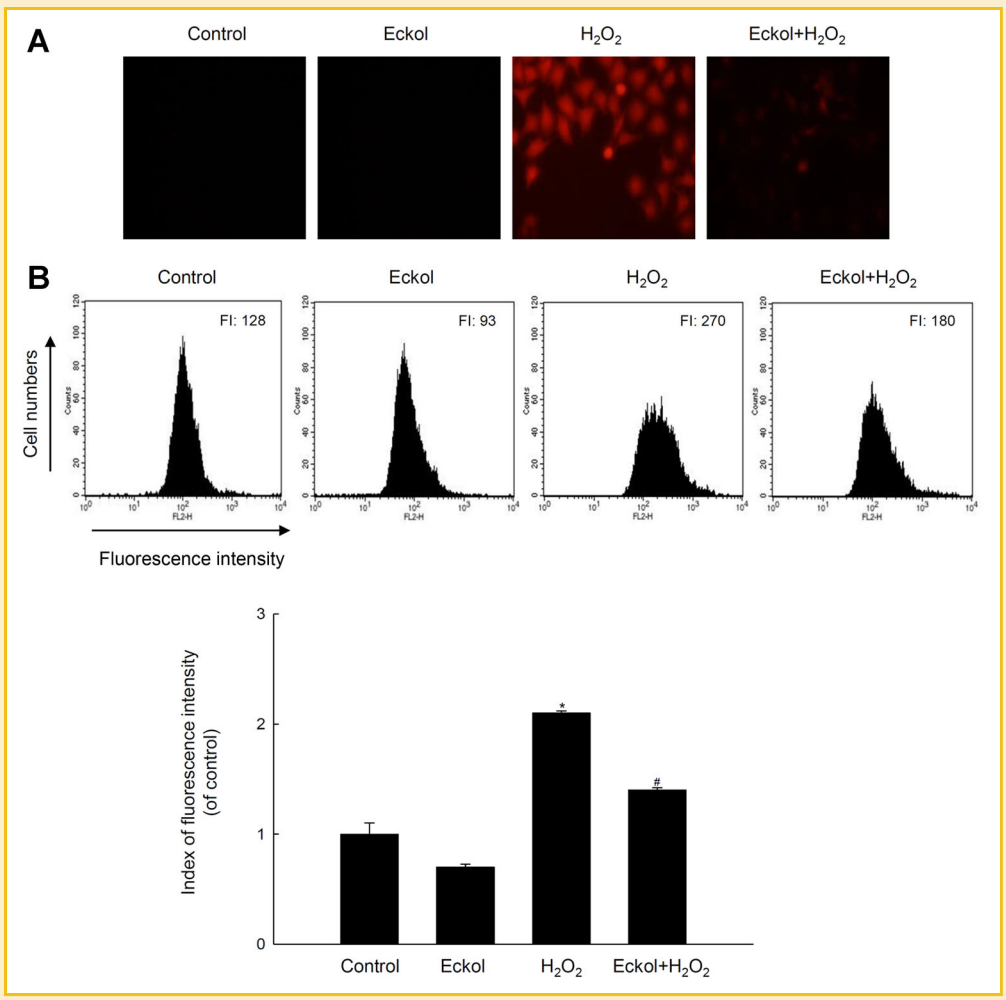

Fig. 2. Effect of eckol on mitochondrial Ca^{2+} levels. A: Cells were treated with eckol for 1 h, followed by H_2O_2 for 24 h. After changing the cell culture medium, Rhod-2 AM was added and the cells were incubated for 30 min at 37°C. Representative confocal images illustrated the increase in the red fluorescence intensity of Rhod-2 AM generated by the increased mitochondrial Ca^{2+} levels in H_2O_2-treated cells compared with the untreated control, eckol-treated, and eckol-pretreated, H_2O_2-treated cells (magnification 400×). B: Mitochondrial Ca^{2+} levels were quantified in harvested cells by flow cytometry. FI indicates fluorescence intensity of Rhod-2 AM.

[Cheng et al., 2012]. Confocal microscopy revealed that eckol decreased the red fluorescence intensity of Rhod-2 AM-stained, H_2O_2-induced mitochondrial Ca^{2+} (Fig. 2A). Moreover, pretreatment of H_2O_2-treated cells with eckol reduced the fluorescence intensity value from 270 (index 2) in H_2O_2-treated cells to 180 (index 1.4), which were detected by using flow cytometry (Fig. 2B).

ECKOL PREVENTS MITOCHONDRIAL DYSFUNCTION FOLLOWING ROS AND CA^{2+} INDUCTION

Excessive mitochondrial ROS and Ca^{2+} levels bring about mitochondrial dysfunction via depletion of ATP, depolarization of mitochondrial action potentials, and permeabilization of mitochondrial membranes [Cheng et al., 2012]. ATP content was lower in H_2O_2-treated cells than in control cells (Fig. 3A). However, eckol pretreatment of H_2O_2-treated cells lessened this decrease in ATP content. Succinate dehydrogenase exists in the mitochondrial respiratory chain of the mitochondrial membrane. Hence, this enzyme is indicative of mitochondrial membrane integrity [Carmichael et al., 1987]. Therefore, succinate dehydrogenase activity was next assessed by using MTT assay. Although H_2O_2 reduced succinate dehydrogenase activity to 55% of the value in control cells, eckol recovered its activity to 74% of the control value (Fig. 3B). Taken together, the observations shown in Figure 3 suggest that eckol safeguards cells against H_2O_2-generated mitochondrial dysfunction by preventing, at least in part, the loss of succinate dehydrogenase activity and mitochondrial ATP.

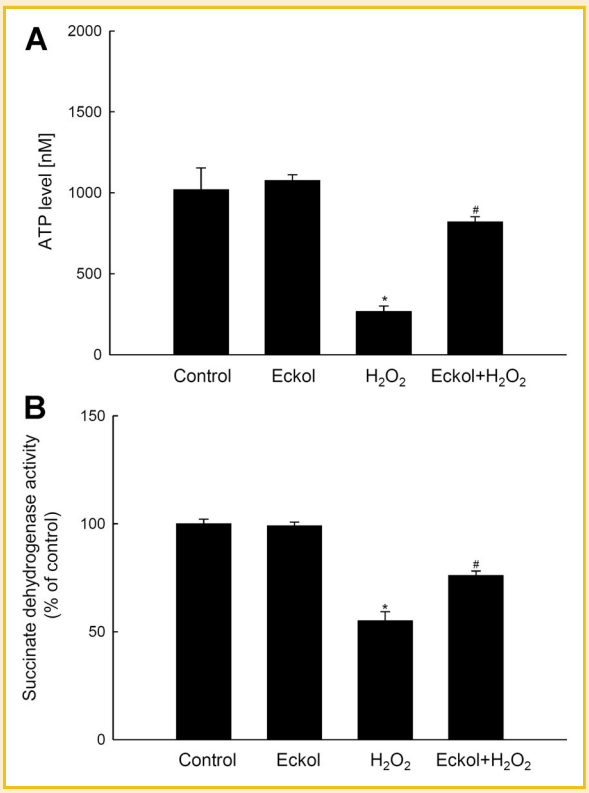

Fig. 3. Effect of eckol on intracellular ATP levels and succinate dehydrogenase activity. A: ATP content was assayed by using a luciferase/luciferin ATP determination kit. *Significantly different from control cells ($P < 0.05$), and #significantly different from H_2O_2-treated cells ($P < 0.05$). B: Succinate dehydrogenase activity was detected via the MTT assay. *Significantly different from control cells ($P < 0.05$), and #significantly different from H_2O_2-treated cells ($P < 0.05$).

ECKOL ENHANCES Mn SOD EXPRESSION AND ACTIVITY

Mn SOD acts as a first defense system to protect mitochondria and other cellular components from oxidative stress by scavenging superoxide anions in the mitochondrial matrix [Fridovich, 1995]. Notably, eckol treatment alone induced Mn SOD mRNA and protein expression in a time-dependent manner (Fig. 4A,B). By contrast, H_2O_2 decreased the expression of Mn SOD protein; however, eckol prevented the H_2O_2-mediated attenuation of expression levels (Fig. 4C). Furthermore, eckol defended cells against the loss of Mn SOD activity in response to H_2O_2 exposure (Fig. 4D).

ECKOL INCREASES Mn SOD EXPRESSION VIA AMPK AND FoxO3a ACTIVATION

We next explored the ability of eckol to activate AMPK and FoxO3a. Eckol increased the phosphorylation of AMPKα (Fig. 5A) and FoxO3a (Fig. 5B) in a time-dependent manner, ultimately resulting in the accumulation of FoxO3a in the nucleus (Fig. 5C). Therefore, we investigated whether FoxO3a and AMPK signaling pathways were involved in the induction of Mn SOD expression by eckol. Cells were transfected with siFoxO3a RNA and treated with eckol 24 h later. The eckol-enhanced expression of Mn SOD was markedly inhibited by siRNA knock down of the FoxO3a gene (Fig. 6A). Furthermore, compound C (an AMPK inhibitor) attenuated Mn SOD expression in eckol-treated cells (Fig. 6B), as did transfection of siAMPK RNA (Fig. 6C). To determine whether eckol-enhanced Mn SOD activity confers cytoprotection against oxidative stress, cells were pretreated with the DEDTC, a Mn SOD inhibitor. DEDTC reduced the protective actions of eckol against H_2O_2-induced cytotoxicity, similar to the effects observed for siMn SOD RNA (Fig. 6D).

DISCUSSION

Marine algae are increasingly recognized as an important source of natural bioactive secondary metabolites, including phenols and polyphenols [Torres et al., 2008]. Phlorotannin components are a type of marine algal polyphenol that are found in particularly high amounts in brown algae [Shibata et al., 2002]. Eckol is an *Ecklonia cava*-derived polymer of phloroglucinol with a polyphenol structure. We previously demonstrated that eckol protects against oxidative stress-induced cell damage via the Erk/nuclear factor κB/catalase signaling pathway [Kang et al., 2005]. In addition, eckol up-regulates heme oxygenase-1 via activation of Erk and phosphoinositide 3-kinase [Kim et al., 2010].

Mitochondria contribute to a variety of essential processes in living cells, such as ATP synthesis by oxidative phosphorylation, ROS production, and Ca^{2+} uptake and release. Of these, the most important process for the maintenance of life is ATP synthesis by oxidative phosphorylation [Pedersen, 1999]. On the other hand,

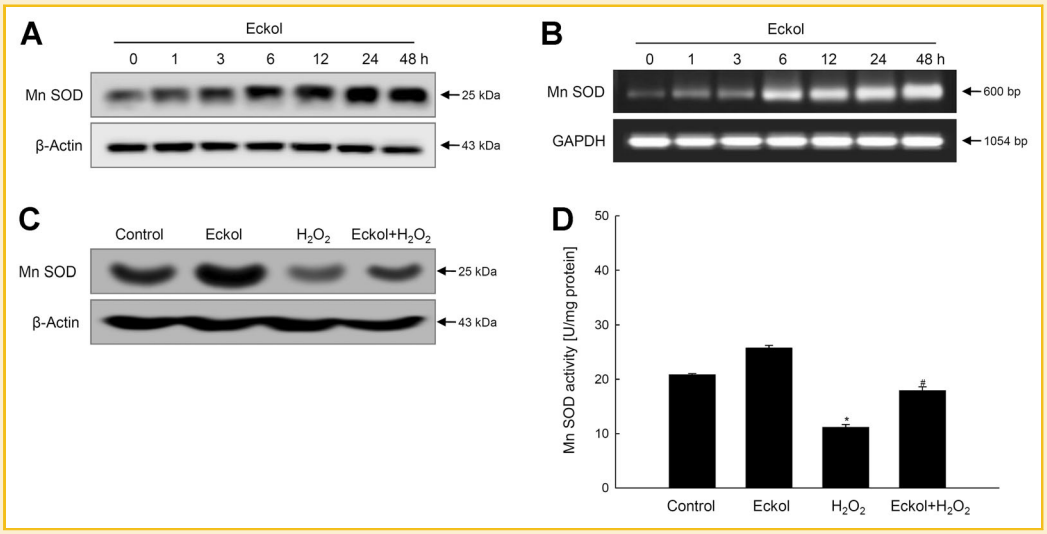

Fig. 4. Effect of eckol on Mn SOD expression and activity. A: Cells were treated with eckol, total RNA was extracted, and Mn SOD mRNA expression was analyzed by RT-PCR. The GAPDH band is shown to confirm RNA integrity and equal RNA loading. B: Cells were treated with eckol for various periods of time, lysed, electrophoresed in SDS–polyacrylamide gels and transferred to nitrocellulose membranes. Mn SOD protein expression was detected via reaction with a specific antibody against Mn SOD. β-Actin was used as a loading control. C: Cells were treated with eckol for 1 h, followed by H_2O_2 for 24 h. Cell lysates were subjected to Western blotting analysis with primary antibodies against Mn SOD and β-actin. D: Mn SOD enzyme activity is expressed as enzyme units per mg protein. *Significantly different from control cells ($P < 0.05$), and #significantly different from H_2O_2-treated cells ($P < 0.05$).

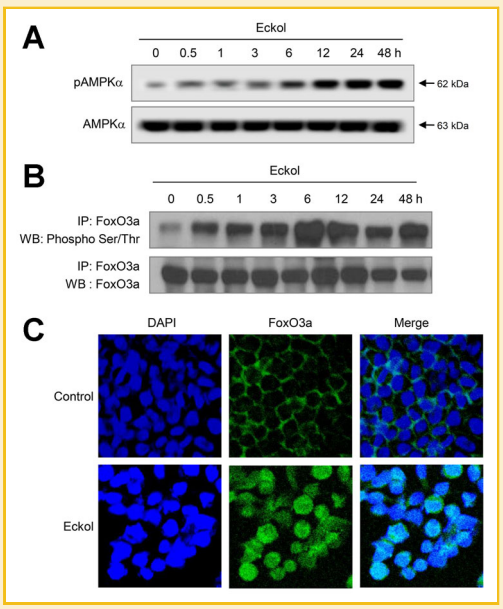

Fig. 5. Effects of eckol on AMPK and FoxO3a phosphorylation and translocation of FoxO3a into the nucleus. A: Cells were treated with eckol for various periods of time. Cell lysates were subjected to Western blotting analysis with primary antibodies against phospho AMPKα and AMPKα. B: Cell lysates were subjected to immune-precipitation with an antibody against FoxO3a, and the immune-precipitates were subjected to Western blotting analysis with an antibody against phospho serine/threonine. C: Cells were labeled with a primary antibody against FoxO3a, followed by a fluorescein-conjugated secondary antibody, and confocal microscopy imaging was used to localize FoxO3a (green). 4′,6-Diamidino-2-phenylindole-stained nuclei are also shown (blue). The merged images demonstrated the nuclear translocation of FoxO3a in eckol-treated cells.

oxidative stress stemming from the excessive generation of ROS and other free radicals can lead to oxidative damage to mitochondrial proteins, lipid membranes, and DNA. Hence, oxidative damage severely impairs the ability of mitochondria to synthesize ATP and carry out their wide range of vital metabolic functions [Madamanchi and Runge, 2007].

A delicate balance between ROS and Ca^{2+} levels also profoundly affects mitochondrial function. Hydrogen peroxide stress leads to superoxide generation due to damage to the electron transport chain [Kirkinezos and Moraes, 2001]. Mitochondrial dysfunction by oxidative stress has been correlated with the liver lesions of non-alcoholic steatohepatitis and cytolytic hepatitis [Pessayre, 2007; Wei et al., 2008]. The current study showed that eckol prevented the induction of mitochondrial ROS by H_2O_2, as well as the resultant ROS-mediated overloading of mitochondrial Ca^{2+} in Chang liver cells. Furthermore, ATP production and succinate dehydrogenase activity were decreased by H_2O_2 in our system, but these actions were largely reversed by eckol. Moreover, mitochondria are the major cellular source of superoxide production [Orrenius, 2007], contributing to oxidative damage under pathological conditions. Mitochondrial superoxides are generally conveyed through a series of electron carriers that are arranged spatially according to their redox potentials, but they are quickly dismutated to the less destructive H_2O_2 and diatomic oxygen by Mn SOD [Shimoda-Matsubayashi et al., 1996]. Of great relevance, eckol increased Mn SOD expression by itself and defended cells against the reduction in Mn SOD expression and activity brought about by exposure to excess H_2O_2.

FoxO3a transcription factor also protects against oxidative stress by increasing the levels of Mn SOD, as well as catalase and the DNA

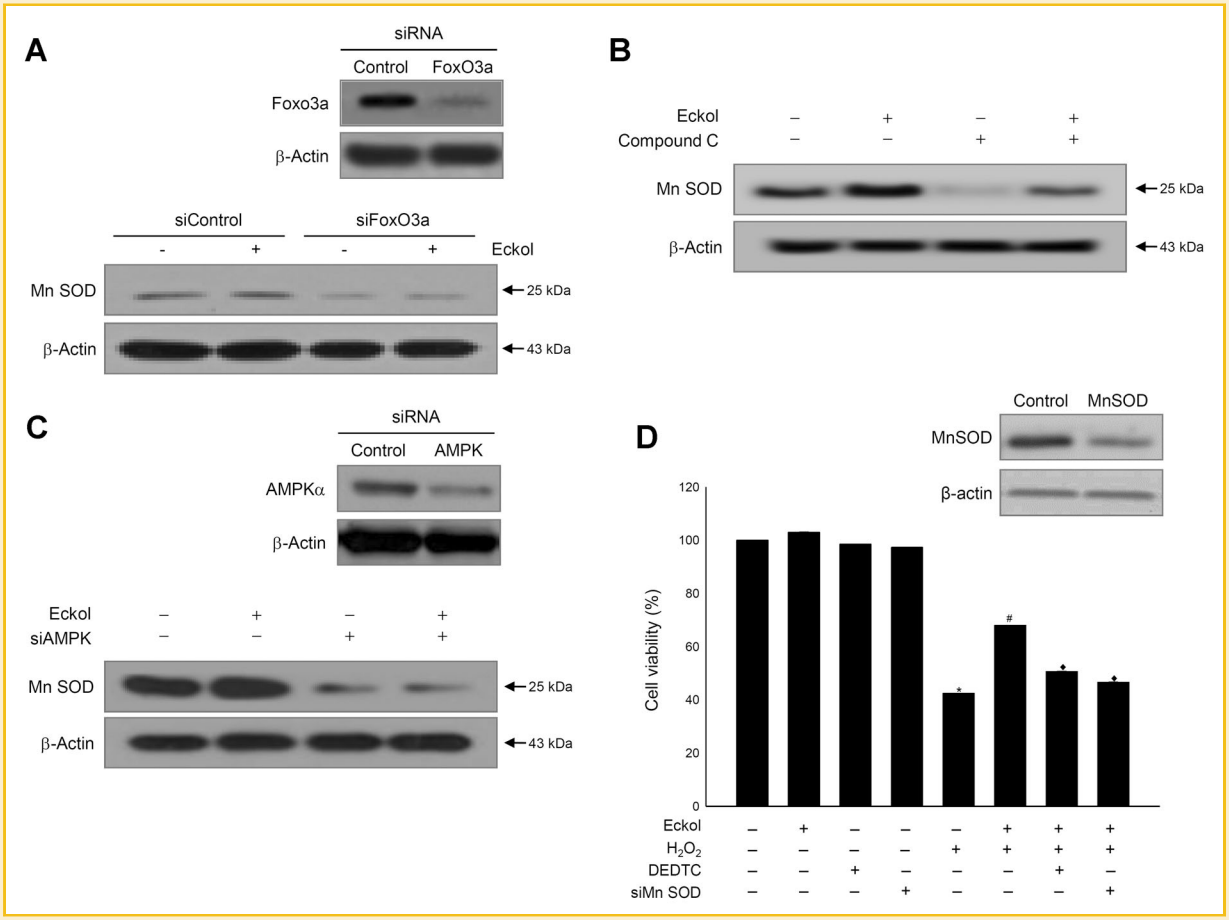

Fig. 6. Induction of Mn SOD by eckol via an AMPK/FoxO3a signaling pathway. A: Cells were transfected with 10–50 nM siControl RNA or siFoxO3a RNA. At 24 h after transfection, the cells were treated with eckol for 24 h. The expression of Mn SOD protein was then evaluated in cell lysates by Western blotting analysis. B: Cells were incubated with eckol in the presence of compound C. Cell lysates were subjected to Western blotting analysis with primary antibodies against Mn SOD and β-actin. C: Cells were transfected with 10–50 nM siControl RNA or siAMPK RNA. At 24 h after transfection, the cells were treated with eckol for 24 h, and the expression of Mn SOD protein was evaluated in cell lysates by Western blotting analysis. D: Cells were transfected with 10–50 nM siControl RNA or siMn SOD RNA. At 24 h after transfection, the cells were pretreated with 10 μM DEDTC for 30 min, followed incubation with eckol for 1 h, and subsequent exposure to H_2O_2 for 24 h. Cell viability was measured by using the MTT assay. *Significantly different from control cells ($P < 0.05$), #significantly different from H_2O_2-treated cells ($P < 0.05$), and ◆significantly different from eckol-pretreated and H_2O_2-treated cells ($P < 0.05$).

repair enzyme [Kops et al., 2002; Tran et al., 2002; Greer et al., 2007]. AMPK is a heterotrimeric FoxO3a regulatory protein comprising two catalytic (α1 and α2) and five different regulatory (β1, 2 and γ1–3) subunits, and functions as a protein serine/threonine kinase. Increasing evidence suggests that AMPK can activate FoxO3a through direct phosphorylation. FoxO3a then translocates into the nucleus and activates Mn SOD and catalase, and down-regulates ROS levels [Hou et al., 2010; Zhao et al., 2011]. Of note, eckol induced the expression of phosphorylated AMPK and FoxO3a in this study and increased the nuclear translocation of FoxO3a, whereas transfection of cells with siAMPK RNA and siFoxO3a RNA decreased Mn SOD protein expression. Thus, induction of Mn SOD by eckol is apparently regulated via the AMPK/FoxO3a pathway. In addition, DEDTC (a potent inhibitor of Mn SOD) and siMn SOD RNA overturned the protective effects of eckol against oxidative stress-induced cell death, providing evidence for a role of Mn SOD in the cytoprotective mechanism of eckol.

In conclusion, eckol attenuated mitochondrial oxidative stress by stimulating AMPK/FoxO3a-mediated Mn SOD expression and activation. These results suggest the possible application of eckol for the amelioration of mitochondrial ROS-related pathological conditions.

ACKNOWLEDGMENTS

This work was supported by a grant from the National Research Foundation of Korea funded by the Korean Government (Ministry of Education, Science and Technology) (grant no. NRF-C1ABA001-2011-0021037).

REFERENCES

Alley MC, Scudiero DA, Monks A, Hursey ML, Czerwinski MJ, Fine DL, Abbott BJ, Mayo JG, Shoemaker RH, Boyd MR. 1988. Feasibility of drug screening

with panels of human tumor cell lines using a microculture tetrazolium assay. Cancer Res 48:589–601.

Balaban RS, Nemoto S, Finkel T. 2005. Mitochondria, oxidants, and aging. Cell 120:483–495.

Banki K, Hutter E, Gonchoroff NJ, Perl A. 1999. Elevation of mitochondrial transmembrane potential and reactive oxygen intermediate levels are early events and occur independently from activation of caspases in Fas signaling. J Immunol 162:1466–1479.

Carmichael J, DeGraff WG, Gazdar AF, Minna JD, Mitchell JB. 1987. Evaluation of a tetrazolium-based semiautomated colorimetric assay: Assessment of chemosensitivity testing. Cancer Res 47:936–942.

Cheng G, Kong RH, Zhang LM, Zhang JN. 2012. Mitochondria in traumatic brain injury and mitochondrial-targeted multipotential therapeutic strategies. Br J Pharmacol 167:699–719.

Colombaioni L, Colombini L, Garcia-Gil M. 2002. Role of mitochondria in serum withdrawal-induced apoptosis of immortalized neuronal precursors. Brain Res Dev Brain Res 134:93–102.

Connop BP, Thies RL, Beyreuther K, Ida N, Reiner PB. 1999. Novel effects of FCCP [carbonyl cyanide p-(trifluoromethoxy)phenylhydrazone] on amyloid precursor protein processing. J Neurochem 72:1457–1465.

Devasagayam TP, Tilak JC, Boloor KK, Sane KS, Ghaskadbi SS, Lele RD. 2004. Free radicals and antioxidants in human health: Current status and future prospects. J Assoc Physicians India 52:794–804.

Fridovich I. 1995. Superoxide radical and superoxide dismutases. Annu Rev Biochem 64:97–112.

Fukuyama Y, Miura I, Kinzyo Z, Mori H, Kido M, Nakayama Y, Takahashi M, Ochi M. 1985. Eckols, novel phlorotannins with a dibenzo-p-dioxin skeleton possing inhibitory effects on α2-macroglobulin from the brown alga *Ecklonia kurome* Okamura. Chem Lett 14:739–742.

Ghaffari S, Jagani Z, Kitidis C, Lodish HF, Khosravi-Far R. 2003. Cytokines and BCR-ABL mediate suppression of TRAIL-induced apoptosis through inhibition of forkhead FOXO3a transcription factor. Proc Natl Acad Sci USA 100:6523–6528.

Greer EL, Oskoui PR, Banko MR, Maniar JM, Gygi MP, Gygi SP, Brunet A. 2007. The energy sensor AMP-activated protein kinase directly regulates the mammalian FOXO3 transcription factor. J Biol Chem 282:30107–30119.

Hou X, Song J, Li XN, Zhang L, Wang X, Chen L, Shen YH. 2010. Metformin reduces intracellular reactive oxygen species levels by upregulating expression of the antioxidant thioredoxin via the AMPK-FOXO3 pathway. Biochem Biophys Res Commun 396:199–205.

Hyun KH, Yoon CH, Kim RK, Lim EJ, An S, Park MJ, Hyun JW, Suh Y, Kim MJ, Lee SJ. 2011. Eckol suppresses maintenance of stemness and malignancies in glioma stem-like cells. Toxicol Appl Pharmacol 254:32–40.

Kang KA, Lee KH, Chae S, Zhang R, Jung MS, Lee Y, Kim SY, Kim HS, Joo HG, Park JW, Ham YM, Lee NH, Hyun JW. 2005. Eckol isolated from *Ecklonia cava* attenuates oxidative stress induced cell damage in lung fibroblast cells. FEBS Lett 579:6295–6304.

Kim KC, Kang KA, Zhang R, Piao MJ, Kim GY, Kang MY, Lee SJ, Lee NH, Surh YJ, Hyun JW. 2010. Up-regulation of Nrf2-mediated heme oxygenase-1 expression by eckol, a phlorotannin compound, through activation of Erk and PI3K/Akt. Int J Biochem Cell Biol 42:297–305.

Kiningham KK, Oberley TD, Lin S, Mattingly CA, St Clair DK. 1999. Overexpression of manganese superoxide dismutase protects against mitochondrial-initiated poly (ADP-ribose) polymerase-mediated cell death. FASEB J 13:1601–1610.

Kirkinezos IG, Moraes CT. 2001. Reactive oxygen species and mitochondrial diseases. Semin Cell Dev Biol 12:449–457.

Kops GJ, Dansen TB, Polderman PE, Saarloos I, Wirtz KW, Coffer PJ, Huang TT, Bos JL, Medema RH, Burgering BM. 2002. Forkhead transcription factor FOXO3a protects quiescent cells from oxidative stress. Nature 419:316–321.

Li XN, Song J, Zhang L, LeMaire SA, Hou X, Zhang C, Coselli JS, Chen L, Wang XL, Zhang Y, Shen YH. 2009. Activation of the AMPK-FOXO3 pathway reduces fatty acid-induced increase in intracellular reactive oxygen species by upregulating thioredoxin. Diabetes 58:2246–2257.

Madamanchi NR, Runge MS. 2007. Mitochondrial dysfunction in atherosclerosis. Circ Res 100:460–473.

Marcus DL, Strafaci JA, Freedman ML. 2006. Differential neuronal expression of manganese superoxide dismutase in Alzheimer's disease. Med Sci Monit 12:BR8–14.

Misra HP, Fridovich I. 1972. The role of superoxide anion in the autoxidation of epinephrine and a simple assay for superoxide dismutase. J Biol Chem 247:3170–3175.

Monsalve M, Olmos Y. 2011. The complex biology of FOXO. Curr Drug Targets 12:1322–1350.

Moon C, Kim SH, Kim JC, Hyun JW, Lee NH, Park JW, Shin T. 2008. Protective effect of phlorotannin components phloroglucinol and eckol on radiation-induced intestinal injury in mice. Phytother Res 22:238–242.

Oberley LW, Buettner GR. 1979. Role of superoxide dismutase in cancer: A review. Cancer Res 39:1141–1149.

Orrenius S. 2007. Reactive oxygen species in mitochondria-mediated cell death. Drug Metab Rev 39:443–455.

Pedersen PL. 1999. Mitochondrial events in the life and death of animal cells: A brief overview. J Bioenerg Biomembr 31:291–304.

Pessayre D. 2007. Role of mitochondria in non-alcoholic fatty liver disease. J Gastroenterol Hepatol 22:S20–S27.

Piao MJ, Lee NH, Chae S, Hyun JW. 2012. Eckol inhibits ultraviolet B-induced cell damage in human keratinocytes via a decrease in oxidative stress. Biol Pharm Bull 35:873–880.

Richter C. 1993. Pro-oxidants and mitochondrial Ca^{2+}: Their relationship to apoptosis and oncogenesis. FEBS Lett 325:104–107.

Shibata T, Yamaguchi K, Nagayama K, Kawaguchi S, Nakamura T. 2002. Inhibitory activity of brown algal phlorotannins against glycosidases from the viscera of the turban shell Turbo cornutus. Eur J Phycol 37:493–500.

Shimoda-Matsubayashi S, Matsumine H, Kobayashi T, Nakagawa-Hattori Y, Shimizu Y, Mizuno Y. 1996. Structural dimorphism in the mitochondrial targeting sequence in the human manganese superoxide dismutase gene. A predictive evidence for conformational change to influence mitochondrial transport and a study of allelic association in Parkinson's disease. Biochem Biophys Res Commun 226:561–565.

Torres MA, Barros MP, Campos SC, Pinto E, Rajamani S, Sayre RT, Colepicolo P. 2008. Biochemical biomarkers in algae and marine pollution: A review. Ecotoxicol Environ Saf 71:1–15.

Tran H, Brunet A, Grenier JM, Datta SR, Fornace AJ , Jr. , DiStefano PS, Chiang LW, Greenberg ME. 2002. DNA repair pathway stimulated by the forkhead transcription factor FOXO3a through the Gadd45 protein. Science 296:530–534.

Wei Y, Rector RS, Thyfault JP, Ibdah JA. 2008. Nonalcoholic fatty liver disease and mitochondrial dysfunction. World J Gastroenterol 14:193–199.

Weisiger RA, Fridovich I. 1973. Superoxide dismutase. Organelle specificity. J Biol Chem 248:3582–3592.

Zhang R, Kang KA, Piao MJ, Ko DO, Wang ZH, Lee IK, Kim BJ, Jeong IY, Shin T, Park JW, Lee NH, Hyun JW. 2008. Eckol protects V79-4 lung fibroblast cells against gamma-ray radiation-induced apoptosis via the scavenging of reactive oxygen species and inhibiting of the c-Jun NH(2)-terminal kinase pathway. Eur J Pharmacol 591:114–123.

Zhang R, Kang KA, Piao MJ, Kim KC, Kim AD, Chae S, Park JS, Youn UJ, Hyun JW. 2010. Cytoprotective effect of the fruits of *Lycium chinense* Miller against oxidative stress-induced hepatotoxicity. J Ethnopharmacol 130:299–306.

Zhao Y, Wang Y, Zhu WG. 2011. Applications of post-translational modifications of FoxO family proteins in biological functions. J Mol Cell Biol 3:276–282.